H.M. Hussein et al. / ICEHM2000, Cairo University, Egypt, September, 2000, page 102- 117

Spectral Analysis and scaling relations of Cairo Earthquake sequence of Oct. 12,1992 recorded at KEG VBB Station

Hussein. H. M.(*) , Farouk M.A.(*)
* *National Research Institute of Astronomy and Geophysics*

Abstract- Spectral analysis of fifty six KEG VBB records from Cairo earthquake source region is preformed to obtain the source parameters such as the seismic moment, source radius and stress drop. These parameters are used in turn to obtain empirical local magnitude (**ML**)- Seismic moment (**Mo**) – Coda duration (**D**) relations for that region.

In this study the data consist of **Lg** waves on the vertical component seismograms for earthquakes of **ML** between **1.7** and **4.7**. The mainshock has a seismic moment (**Mo**) of **1.37 x 10^{24} dyne.cm** , a source radius of **1.3 km** and stress drop of **270 bar**.

For the aftershock sequence, the derived empirical relation between the seismic moment (**Mo**) and **ML** for magnitude range 1.7<**ML**<4.7 is

$$\mathbf{Log\ (Mo) = (0.96\pm0.2)\ ML + (17.89\pm0.56)}$$

Stress drops of the events under study lies in the range between (0.12 –120 bar). It tends to increase with increasing seismic moment in the range less than 10^{21}dyne.cm but appear to be constant at greater values. The estimated source radius in nearly constant.

Radiated energy released (**Es**) were calculated for these aftershocks from the shear wave velocity time series. The radiated energy is related with seismic moment and local magnitude by:

$$\mathbf{Log\ (Es) = (1.752\ \pm0.03)\ ML + (12.86\ \pm0.09)}$$
$$\mathbf{Log(Es) = (1.74\ \pm0.059)\ Log(Mo) – (18.07\pm1.2)}$$

1-Introduction

On the 12th of October 1992 a moderate Size earthquake of **M_w=5.8** occurred at epicentral distance of about **25 Km** south west of the Cairo city in Dahshour region at a depth of **22** km (**Fig1**). This earthquake was felt from Alexandria to Aswan. It registered a maximum observed intensity of **7** in **MSK** intensity scale in Dahshour region. This shock caused considerable damage to the buildings in four districts: Eastern part of Cairo, Giza and its suburb and Northern area of Fayoum. Significant damage was found mostly in adobe or old non-reinforced brick masonry buildings and non-engineering reinforced concrete building. In addition extensive liquefaction of deltaic silty sand deposits was observed in some villages of Giza City located **19 km** from the epicenter. According to eyewitness sand and water continuously below up to a height of **3 m** for about **45** minutes.

The Cairo earthquake has struck in a previously low seismicity area. The only significant earthquake reported in this region during the historical period occurred in 1847. The mainshock was followed by aftershocks activity. Within twenty two days after the occurrence of Cairo earthquake 55 shocks with **1.7<ML<4.7** were recorded by KEG Broad Band station. Event data are given in **table 1**. **Fig (2)** shows the distribution of the well located aftershocks of the Cairo earthquake sequence of 1992 recorded by a temporary seismic network installed by National Research Institute of Astronomy and Geophysics during the first twenty days of this sequence. Details about the seismic network and procedure of determination the hypocenters are given by Abou El enein,et al. 1999. The pattern of the aftershocks reflects a cluster rather than a clear trend of seismicity.

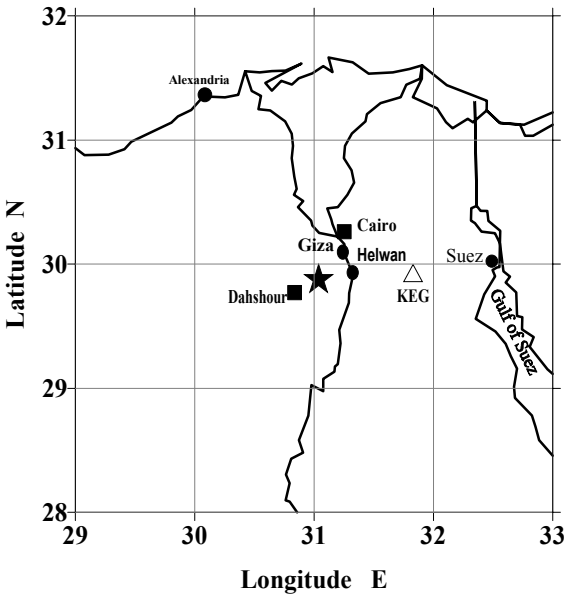

Figure (1): Dahshour area and its location related to Cairo city.

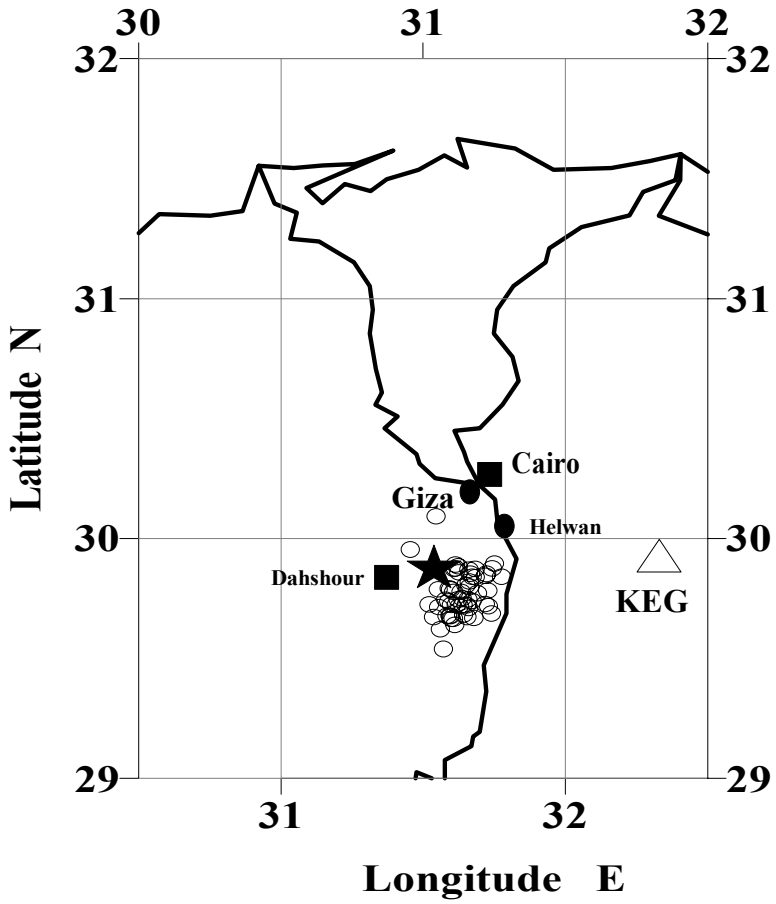

Fig (2): Dahshour aftershocks distributions.

Table (1): ***Hypocentral locations of the events under study as the result of the Hypo71 software.***

#	Date Y M D	Origin Time H m s	Lat° N	Lon° E	Depth(Km)	MD (HLW)	ML
1	921012	13 9 55.87	29-50.83	31- 2.29	23.20	5.3	5.96
2	921012	13 50 9.65	29-46.94	31-13.66	10.93		2.52
3	921012	14 11 8.64	29-43.33	31- 9.12	18.84		2.31
4	921012	14 15 7.43	29-57.23	30-57.28	25.09		2.81
5	921012	14 58 14.73	29-52.55	31-14.55	22.32		1.84
6	921012	15 07 42.05	29-53.52	31- 6.80	26.85		2.34
7	921012	15 25 24.65	29-52.48	31- 6.83	29.55		4.7
8	921012	15 52 50.77	29-51.24	31- 9.94	22.77		2.26
9	921012	16 55 9.79	29-50.29	31-11.01	25.59		2.37
10	921012	18 31 42.36	29-47.89	31- 9.82	21.14		2.24
11	921012	19 55 59.20	29-51.15	31-13.38	19.10		2.19
12	921012	21 31 34.22	29-40.00	31- 7.06	20.73		4.15
13	921012	21 46 16.02	29-43.61	31-13.10	9.83	2.9	2.45
14	921012	23 34 22.50	29-55.72	31-16.90	17.10	3.0	2.69
15	921012	23 46 24.42	29-44.40	31-10.38	21.78	2.9	2.13
16	921013	18 09 8.14	29-52.44	31-10.98	22.39	3.4	3.67
17	921013	18 34 54.26	29-50.62	31-13.15	20.72		3.16
18	921013	23 27 56.39	29-53.00	31- 7.37	32.02	2.4	2.22
19	921014	02 44 23.14	29-52.16	31- 9.69	30.25	3.1	2.77
20	921014	03 50 14.53	29-46.63	31- 6.43	29.49	3.4	2.76
21	921014	09 40 27.04	29-43.49	31- 1.28	27.64	4.0	4.17
22	921014	10 4157.34	29-46.67	31- 7.99	22.95	2.6	1.94
23	921014	12 09 15.72	29-43.34	31- 5.99	20.53		2.95
24	921014	13 46 39.47	29-50.45	31-10.37	28.51	3.5	3.22
25	921014	14 23 44.67	29-41.18	31-14.42	20.22	3.1	2.4

#	Date Y M D	Origin Time H m s	Lat° N	Lon° E	Depth(Km)	MD (HLW)	ML
26	921014	14 31 27.90	29-43.41	31- 6.98	24.97	3.3	2.92
27	921014	20 16 11.05	29-49.25	31- 9.74	20.94	2.6	2.29
28	921015	12 13 41.41	29-48.25	31- 9.02	25.52	2.6	1.96
29	921016	03 28 51.46	29-47.29	31- 5.79	24.12	2.5	1.99
30	921016	05 56 11.84	29-47.31	31- 3.17	30.70	3.1	2.91
31	921016	09 57 46.87	29-47.50	31- 5.51	26.25	3.3	3.08
32	921016	18 07 53.12	29-51.50	31- 7.49	24.20	2.6	2.4
33	921017	01 35 28.51	29-45.06	31- 8.25	25.44	2.6	2.03
34	921018	08 12 16.12	29-43.38	31- 8.40	20.74	3.4	2.86
35	921018	13 04 28.44	29-42.75	31-13.80	18.50	3.0	2.61
36	921019	10 46 30.95	29-42.67	31- 9.58	21.58	2.9	2.23
37	921019	12 30 16.44	29-44.22	31- 6.30	25.20	3.2	2.99
38	921019	14 59 50.43	29-44.50	31- 8.87	18.68	3.3	3.17
39	921020	06 00 30.77	29-32.36	31- 4.27	22.28	2.7	1.65
40	921020	17 28 28.44	29-40.39	31- 9.24	20.62	2.5	1.98
41	921020	23 14 47.46	29-43.08	31- 7.65	17.20	3.1	3.11
42	921021	18 09 27.53	29-46.47	31-12.00	14.65	2.7	1.97
43	921022	08 28 58.70	29-44.83	31- 6.53	21.90	3.4	3.42
44	921022	17 38 57.30	29-40.62	31- 5.68	22.88	3.9	4.59
45	921023	02 40 5.43	29-44.21	31- 5.46	22.85	2.6	2.17
46	921023	15 12 10.08	29-41.39	31-10.00	22.40	3.8	3.29
47	921023	16 02 4.12	29-44.78	31- 7.38	21.70	2.4	1.7
48	921025	09 05 4.64	29-40.09	31-10.71	22.05	3.1	2.8
49	921025	12 26 15.06	29-39.93	31- 5.95	24.12	3.1	2.72
50	921025	16 21 05.28	29-38.35	31- 6.70	22.92	2.9	2.31
51	921025	19 45 34.56	29-40.97	31- 8.52	23.78	2.3	3.16

#	Date Y M D	Origin Time H m s	Lat° N	Lon° E	Depth(Km)	MD (HLW)	ML
52	921026	06 45 23.96	29-52.40	31- 6.49	27.45	3.4	3.27
53	921026	08 43 52.01	29-40.55	31- 5.75	28.25	2.8	2.41
54	921028	06 20 54.90	29-37.30	31- 3.63	24.63	2.9	2.51
55	921028	18 25 56.28	29-50.64	31-16.07	19.46	2.8	2.45
56	921030	14 08 11.19	29-40.70	31- 5.09	25.71	3.0	2.74

Teleseismic body wave inversion of the mainshock (Hussein,1999) suggest normal faulting mechanism with a small strike slip component on a plane striking E-W to WNW-ESE and dipping to the east. (**Fig(3))**

The main objective of this study is to calculate the source parameters of the Cairo earthquake aftershocks recorded by the KEG Broad Band station during three weeks after the mainshock. In addition to develop scaling laws between spectral parameters (Seismic moment, Source radius and Stress drop) and time domain parameters (Coda length) and ML

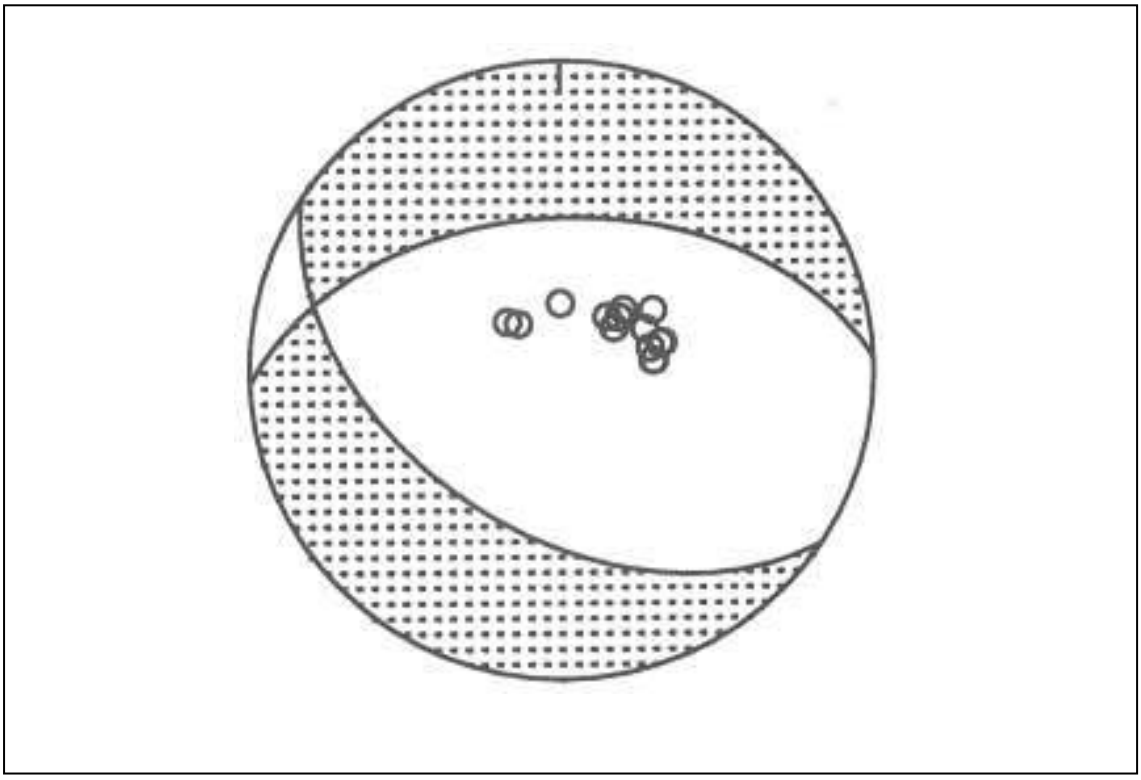

Fig(3) : Fault plane solution of the mainshock

2- Data:

The 55 Dahshour aftershocks recorded during the two weeks after the occurrence of the mainshock of Oct 12,1992 earthquake were selected for the analysis. Event data are given in **Table (1).** The local magnitude (**ML**) of these events varied from 1.7 to 4.7. All of these earthquakes are of crustal origin. Seismic moment, source dimensions and radiated seismic energy were estimated from the digital records of KEG Broad Band station. KEG station is a part of the MEDNET project (Boschi et al, 1988). The seismic records were electronically digitized at a rate of 20 samples per second by **STS-1 VBB** velocity type sensor. For frequencies between 0.003 and 7 HZ the velocity response is flat with a full dynamic range of 140 dB.

3- Method of analysis:

In this work a time window that started shortly before the **Lg** arrival, depending on the size of earthquake was obtained from the vertical component. The time window was nearly 10 sec. long. The digital data within the time window were corrected for the instrumental response, Fourier transformed to obtain the amplitude spectra and then integrated to obtain the displacement spectra. Typical spectrum examples are shown in **Fig (4)**.

The spectrum was corrected for the attenuation, multiplying it by the transfer function $\mathbf{e}^{-\gamma \mathbf{r}}$ where **r** is the distance from the source to the receiver and **γ** is the coefficient of anelastic attenuation which is related to quality factor **Q** (Nuttli, 1986) by :

Where **f** is the wave frequency and **U** is the Lg wave group velocity. Dessoky et al, 1999 obtain a value of **0.001495 km^{-1}** for **1** Hz **Lg** in Dahshour region.

From the corrected spectrum, the low frequency spectral level and the corner frequency were estimated. The low frequency level **(Ωo)** was estimated visually by fitting a straight line at the

$$\gamma = \frac{\pi . f}{U . Q} \qquad (1)$$

low frequency spectra. The corner frequency **(fc)** values were estimated by direct measurements of the low and high frequency trends of the spectra plotted in a double logarithmic scale.

The seismic moment **(Mo)** were derived for the 55 recorded events from the low spectral level **(Ωo)** estimated using street et al., 1975 formula that was subsequently derived by means of theoretical modeling by Herrmann and Kyko, 1983

$$\mathbf{Mo = 4\Pi\rho\beta^3\ Ro\ (R/Ro)\ \ \Omega o \qquad R<Ro \qquad (2)}$$
$$\mathbf{Mo = 4\Pi\rho\beta^3\ Ro\ (R/Ro)^{1/2}\ \Omega o \qquad R<Ro}$$

Where **ρ** is the density of the medium, **β** is the shear wave velocity, **R** is the epicentral distance and **Ro** is a reference distance. The reference distance **Ro** was determined empirically by comparing values of seismic moment given by the above relation with those obtained by amplitude equalization of long period surface wave (e.g. from Hermann, 1974).

For a circular fault the source radius **ro** can be calculated from the corner frequency, with Brune's, (1970) relation:-

$$r_o = \frac{2.34\beta}{2\Pi f_c} \qquad (3)$$

Typical source radius values ranges from **0.26** to **0.65 km**.

The stress drop **Δδ** is given by the following relation (Keilis-Borok,1959; Brune,1970).

The estimated stress drop varied from 0.12 to 120 bars. In this work radiated energy was also calculated following Boatwright (1980). The following equation was used to calculate the

$$\Delta\delta = \frac{0.44 Mo}{r_o^3} \qquad (4)$$

radiated seismic energy in the body wave arrivals.

$$Es = \left(\frac{R}{FR_{\theta\phi}}\right)^2 . \frac{\rho(r)\beta(r)}{e(\theta,\phi)} I \qquad (5)$$

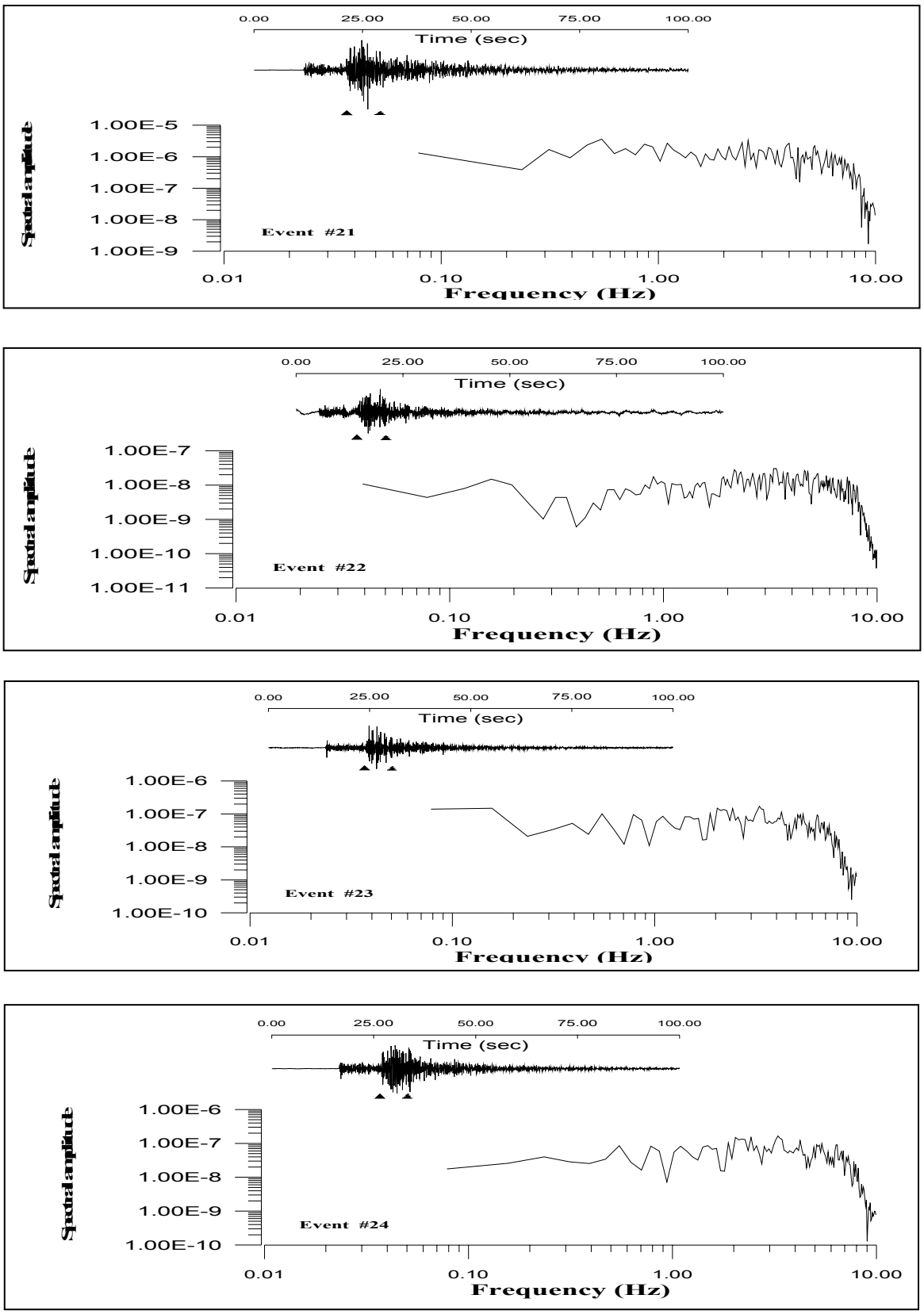

Fig (4): FFT spectrum of some selected events

Where **R** is the hypocentral distance, **F** is the free surface correction, $\mathbf{R_{\theta,\varphi}}$ is the radiation pattern coefficient, **ρ(r),β(r)** are the density and the shear wave velocity at the receiver respectively, **e(θ,φ)** is the fractional Energy flux and **I** is the integral of the square of the ground velocity and it is expressed as follows:

$$I = \int_0^\infty \overset{o}{U}(r,t)dt = \frac{1}{\Pi}\int_0^\infty \left|\overset{o}{U}\right|^2 d\omega \qquad (6)$$

Where U(r,w) is the velocity spectrum.

The fractional energy flux relates the shear wave energy flux at a particular take off angle with the total radiated seismic energy.

The horizontal components for the selected aftershocks were rotated into their radial and transverse components before calculation in order to get reliable results. The Integral of the square of the ground velocities were taken from the KEG record after doing the appropriate analysis and squaring and take the appropriate window. The parameters calculated using the above formulas are listed in **table (2)**

Results:

1.1 Seismic moment coda duration and local magnitude

The seismic moments of the events under study were estimated using **equation (2)**. Constant values corresponding to Dahshour region in **equation (2)** were selected as follows: **ρ=2.7 gm/cm^3**, **β=3.5 km/sec** and **Ro=100 km**. The seismic moments estimated was found to range from **2.26x10^{22}** to **2.8x10^{19} dyne.cm**. **Table(2)** show the resulted seismic moment as given in this study.

Mathematical regression between the reported seismic moments and the corresponding coda duration has been also done. The Coda duration used in this study were given from the available analog seismographic stations installed in the time of earthquake. It has been taken from the **P** arrival to the point in the coda where the seismic amplitude is nearly twice the background noise amplitude. The Linear regression fitting of the data as shown in **Fig(5)** indicates the following relation:

$$\mathbf{Log(Mo)=(2.42 \pm 0.72)\ Log(D) + (16.21 \pm 1.32)} \qquad \mathbf{(7)}$$

The seismic moment – local magnitude relation is shown in **Fig(6)**. The least square fit implies the following equation:

$$\mathbf{Log\ (Mo) = (0.96\pm0.2)ML + (17.89\pm0.56) \qquad (1.7<ML<4.7) \qquad (8)}$$

This relation is almost similar to that found in Mammoth lakes, California (**Archuleta et al., 1982**) where

$$\mathbf{Log\ (Mo) = (1.05\pm0.08)ML + (17.76\pm0.33) \qquad (\ 0.5 < ML < 6.5) \qquad (9)}$$

Baukun and Lindah (1977) obtained the following relation for earthquake located near Oroville,California

$$\mathbf{Log\ (Mo) = (1.21\pm0.03)ML + (17.02\pm0.07) \qquad (\ 0 < ML < 6) \qquad (10)}$$

Which is also similar to **equation (8)**

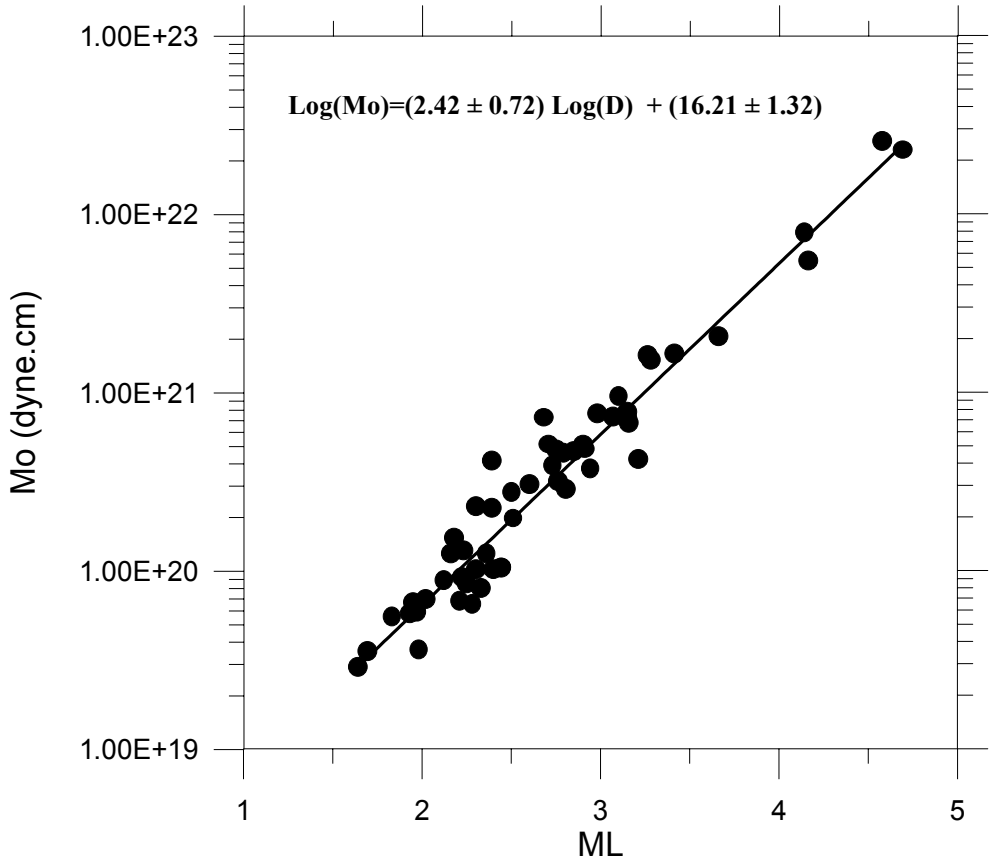

Fig(5): Seismic moment (Mo) - Coda duration relation of Dashshour earthquake sequence

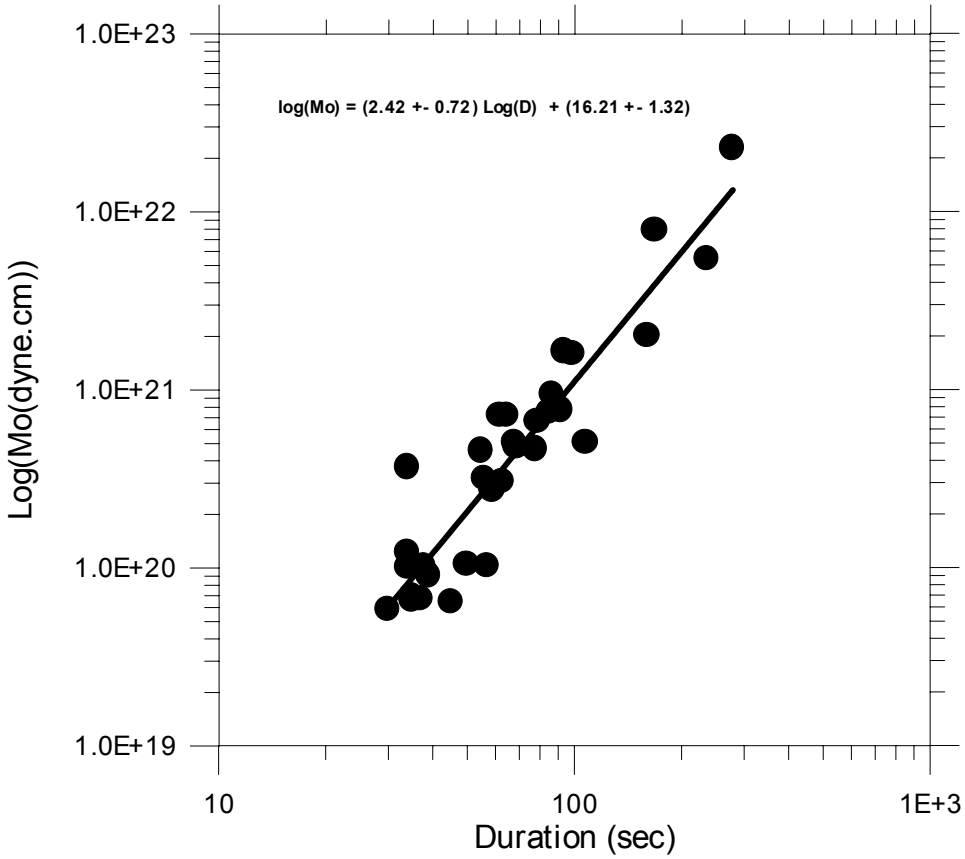

Fig(6): Seismic moment – Local magnitude relation

Table(2): Seismic moment, Stress drop, Source radius of the events under study.

Event #	Duration (sec)	ML	Mo (dyne.cm)	Stress drop (bar)	r0 (km)
1	1040	5.96	1.370604E+24	270.3445	1.30414
2		2.52	1.942783E+20	2.452504	0.326035
3		2.31	2.267175E+20	1.917319	0.3726115
4		2.81	2.836813E+20	3.581097	0.326035
5		1.84	5.468023E+19	0.6902648	0.326035
6		2.34	7.922314E+19	0.1250108	0.65207
7	279	4.7	2.267175E+22	120.7408	0.4347134
8		2.26	8.386375E+19	0.2584638	0.4347134
9		2.37	1.225617E+20	0.6527153	0.4347134
10		2.24	1.28611E+20	1.183562	0.3622611
11		2.19	1.520192E+20	2.221526	0.3105096
12	169	4.15	7.825914E+21	98.79171	0.326035
13	57	2.45	1.021348E+20	1.289315	0.326035
14	65	2.69	7.1504E+20	9.026424	0.326035
15		2.13	8.689964E+19	0.4627932	0.4347134
16	161	3.67	2.028367E+21	17.15362	0.3726115
17	92	3.16	7.671786E+20	4.08569	0.4347134
18	37	2.22	6.70293E+19	0.8461553	0.326035
19	56	2.77	3.1557E+20	3.983649	0.326035
20		2.76	4.717935E+20	5.955762	0.326035
21	237	4.17	5.429151E+21	68.53578	0.326035
22		1.94	5.667937E+19	0.7155013	0.326035
23	34	2.95	3.666106E+20	1.952423	0.4347134
24		3.22	4.157197E+20	2.213959	0.4347134
25		2.4	4.071058E+20	3.442838	0.3726115
26	69	2.92	4.769604E+20	2.540103	0.4347134
27	45	2.29	6.387174E+19	0.3401557	0.4347134
28	35	1.96	6.550127E+19	0.5539353	0.3726115
29		1.99	3.571662E+19	0.8806145	0.260828
30	108	2.91	5.07458E+20	6.405979	0.326035
31	62	3.08	7.187676E+20	3.827873	0.4347134
32		2.4	2.237957E+20	1.191848	0.4347134
33	35	2.03	6.845436E+19	0.5789092	0.3726115
34	78	2.86	4.614945E+20	5.825751	0.326035
35	63	2.61	3.037181E+20	3.834035	0.326035
36	39	2.23	9.024836E+19	0.4806272	0.4347134
37	85	2.99	7.510935E+20	9.481552	0.326035
38	79	3.17	6.659202E+20	5.631596	0.3726115
39		1.65	2.856025E+19	0.360535	0.326035
40	30	1.98	5.832978E+19	0.7363355	0.326035
41	87	3.11	9.421127E+20	5.017321	0.4347134
42		1.97	6.235795E+19	0.5273526	0.3726115
43	94	3.42	1.637872E+21	8.72266	0.4347134
44		4.59	2.522325E+22	118.4098	0.4075438
45	34	2.17	1.227609E+20	0.6537762	0.4347134
46		3.29	1.490997E+21	7.940462	0.4347134
47		1.7	3.499786E+19	0.2959721	0.3726115
48	55	2.8	4.527036E+20	2.410921	0.4347134
49	68	2.72	5.052129E+20	2.690565	0.4347134
50	38	2.31	1.011922E+20	0.8557686	0.3726115
51		3.16	7.076904E+20	3.76888	0.4347134

Event #	Duration (sec)	ML	Mo (dyne.cm)	Stress drop (bar)	r0 (km)
52	99	3.27	1.602396E+21	8.533729	0.4347134
53	34	2.41	1.00893E+20	1.273639	0.326035
54	59	2.51	2.729787E+20	0.4307489	0.65207
55	50	2.45	1.03903E+20	0.5533464	0.4347134
56		2.74	3.834036E+20	2.041856	0.4347134

1.2 Seismic moment,Source radius and Stress drop relationships:

The scaling relation between the seismic moment and source radius is shown in **Fig(7).** Most of earthquakes in this study have stress drops between 0.1 and 10 bars. Source radii ranges from 0.26 to 0.65 km. Events of seismic moment less than 10^{21}dyne.cm have nearly constant source radii that corresponds to decreasing of stress drop with seismic moment decrease the thing that has been observed in several recent strudies (e.g. Kim et al,1989 and Valdes and Meger,1996,Dysart et al.,1988). Asperities and barriers are the physical basis of this phenomena where the slip varies more than one order of magnitude while the fault length remains constant.

For Events of seismic moment greater than 10^{21} dyne.cm, although, there is not enough data that lie in this range, it seems that there is increase of source radius with increase seismic moment while the stress drop remain constant.

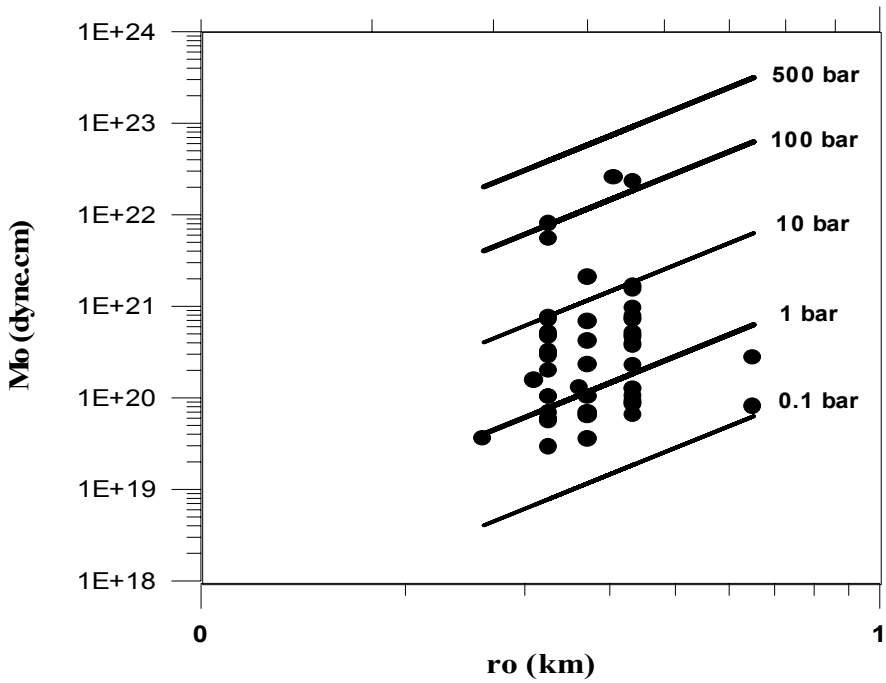

Fig (7): Seismic moment – Stress drop relationship

Radiated Energy relationships

The radiated energies of both the SH and SV velocity time series from the window previously used in the Fourier analysis was obtained from Equation (5)

In this analysis we used $R_{\theta,\varphi}$**=0.6, β=5.5 Km/sec, ρ=2.7 gm/cm^3, f=2 and e(θ,φ)=1/2Π (**based on randall,1973**).**

The resulting estimates of the radiated seismic energy for both radiated and transverse components are compiled in table

The mathematical fitting between the local magnitude (ML) and the average radiated energy estimated in this study is shown in **Fig (8)** the corresponding empirical relation in given by:

$$\text{Log (E)} = (1.752 \pm 0.03)\ \text{ML} + (12.86 \pm 0.09) \qquad (11)$$

Fig(10) Shows the Seismic moment values of the given earthquakes plotted versus their corresponding average radiated energy, the derived equation is as follows:

$$\text{Log (Es)} = (1.74 \pm 0.059)\ \text{Log (Mo)} - (18.07 \pm 1.2) \quad (12)$$

Table(3): Radiated energy values of the events under study.

#	ML	I (rad)	I (trans)	Es(rad) erg	Es(trans) erg	E(average) erg
1	5.96	1.5	3	8.405E+23	1.681E+24	1.26075E+24
2	2.52	0.0000008	0.0000009	2.42406E+17	2.727067E+17	2.575563E+17
3	2.31	4E-8	0.0000004	1.60083E+16	1.60083E+17	8.804565E+16
4	2.81	0.000001	0.0000015	5.950209E+17	8.925313E+17	7.437761E+17
5	1.84	5.5E-8	2E-8	1.483905E+16	5.396017E+15	1.011753E+16
6	2.34	0.0000002	0.0000015	7.981066E+16	5.9858E+17	3.391953E+17
7	4.7	0.0025	0.00215	1.000519E+21	8.604462E+20	9.304826E+20
8	2.26	1.4E-7	1.1E-7	4.868686E+16	3.825396E+16	4.347041E+16
9	2.37	0.0000003	0.0000003	9.954025E+16	9.954025E+16	9.954025E+16
10	2.24	1.6E-7	0.0000002	5.790413E+16	7.238017E+16	6.514215E+16
11	2.19	1.75E-7	2.2E-7	5.093681E+16	6.403485E+16	5.748583E+16
12	4.15	0.0003	0.00029	1.540563E+20	1.48921E+20	1.514887E+20
13	2.45	0.0000003	4.25E-7	9.954025E+16	1.410153E+17	1.202778E+17
14	2.69	0.0000015	0.0000012	3.906013E+17	3.12481E+17	3.515411E+17
15	2.13	8.5E-8	8E-8	3.151297E+16	2.965926E+16	3.058612E+16
16	3.67	0.00005	0.0000475	1.638037E+19	1.556136E+19	1.597086E+19
17	3.16	0.0000075	0.0000055	2.2201E+18	1.628073E+18	1.924087E+18
18	2.22	1.3E-7	2.5E-7	5.06844E+16	9.747E+16	7.40772E+16
19	2.77	0.0000016	1.25E-6	5.59872E+17	4.374E+17	4.98636E+17
20	2.76	0.0000015	1.65E-6	6.444051E+17	7.088455E+17	6.766253E+17
21	4.17	0.0004	0.00025	2.20323E+20	1.377019E+20	1.790125E+20
22	1.94	4E-8	5.5E-8	1.60083E+16	2.201142E+16	1.900986E+16
23	2.95	0.0000013	1.25E-6	5.948377E+17	5.719594E+17	5.833985E+17
24	3.22	0.00001	0.0000085	3.424008E+18	2.910407E+18	3.167208E+18
25	2.4	0.0000004	0.0000005	1.318803E+17	1.648504E+17	1.483654E+17
26	2.92	0.0000025	0.0000026	1.095052E+18	1.138854E+18	1.116953E+18
27	2.29	1.8E-7	1.9E-7	6.435375E+16	6.792896E+16	6.614135E+16
28	1.96	4.5E-8	4.5E-8	1.683375E+16	1.683375E+16	1.683375E+16
29	1.99	3.9E-8	4E-8	1.703572E+16	1.747253E+16	1.725412E+16
30	2.91	0.0000025	0.0000019	1.222408E+18	9.290303E+17	1.075719E+18
31	3.08	0.0000037	0.000004	1.634117E+18	1.766614E+18	1.700366E+18
32	2.4	0.0000004	4.5E-7	1.564083E+17	1.759594E+17	1.661838E+17
33	2.03	5.5E-8	6.5E-8	2.226624E+16	2.631465E+16	2.429045E+16
34	2.86	0.000002	0.0000025	8.260267E+17	1.032533E+18	9.292799E+17
35	2.61	8.5E-7	0.0000009	2.775788E+17	2.93907E+17	2.857429E+17
36	2.23	0.0000001	1.1E-7	3.9675E+16	4.36425E+16	4.165875E+16
37	2.99	0.0000035	0.000005	1.671393E+18	2.387704E+18	2.029549E+18
38	3.17	3.25E-6	2.75E-6	1.252333E+18	1.059667E+18	1.156E+18
39	1.65	1.25E-8	1.5E-8	7.526042E+15	9.03125E+15	8.278646E+15
40	1.98	4E-8	4.5E-8	1.68507E+16	1.895704E+16	1.790387E+16
41	3.11	0.000005	0.0000068	2.142037E+18	2.913171E+18	2.527604E+18
42	1.97	5.5E-8	1.5E-7	1.883204E+16	5.136013E+16	3.509608E+16
43	3.42	0.000013	0.000015	7.23113E+18	8.343612E+18	7.787371E+18
44	4.59	0.0017	0.0022	8.22579E+20	1.064514E+21	9.435465E+20
45	2.17	0.0000001	9E-8	4.6128E+16	4.15152E+16	4.38216E+16
46	3.29	0.000011	0.000011	5.183786E+18	5.183786E+18	5.183786E+18

47	1.7	1.5E-8	1.5E-8	6.319012E+15	6.319012E+15	6.319012E+15
#	ML	I (rad)	I (trans)	Es(rad) erg	Es(trans) erg	E(average) erg
48	2.8	0.000002	0.0000018	7.981066E+17	7.182959E+17	7.582012E+17
49	2.72	0.0000011	1.35E-6	5.336549E+17	6.549402E+17	5.942976E+17
50	2.31	1.4E-7	1.7E-7	6.809787E+16	8.269028E+16	7.539408E+16
51	3.16	0.0000046	0.0000057	1.976175E+18	2.448739E+18	2.212457E+18
52	3.27	0.000018	0.000015	7.329016E+18	6.107513E+18	6.718265E+18
53	2.41	0.0000005	0.0000001	2.41935E+17	4.8387E+16	1.45161E+17
54	2.51	2.75E-7	3.6E-7	1.529662E+17	2.002467E+17	1.766064E+17
55	2.45	1.6E-7	1.3E-7	3.93132E+16	3.194197E+16	3.562759E+16
56	2.74	5.5E-7	0.0000006	2.724521E+17	2.972205E+17	2.848363E+17

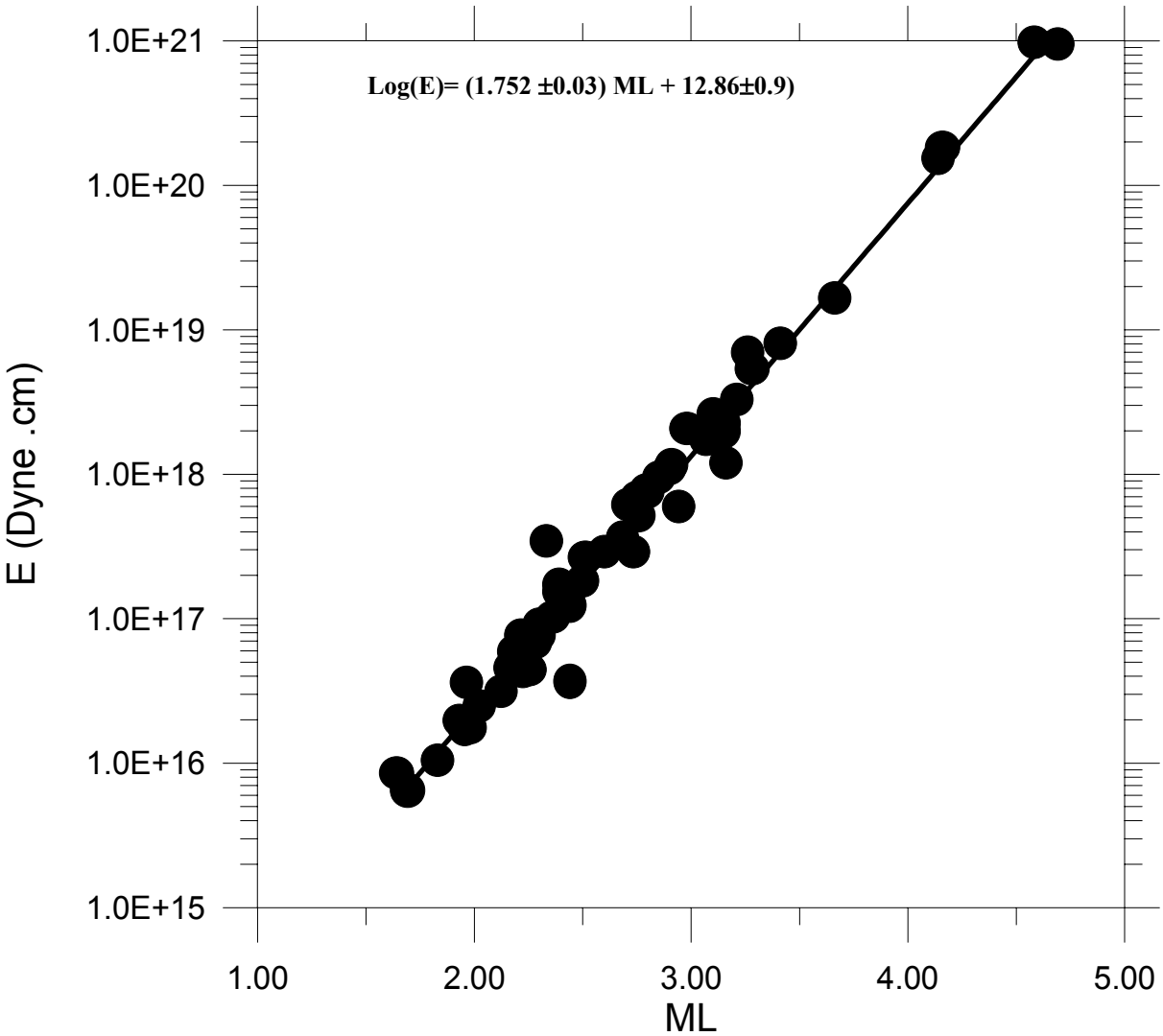

Fig(9): Average Energy – ML Relationship.

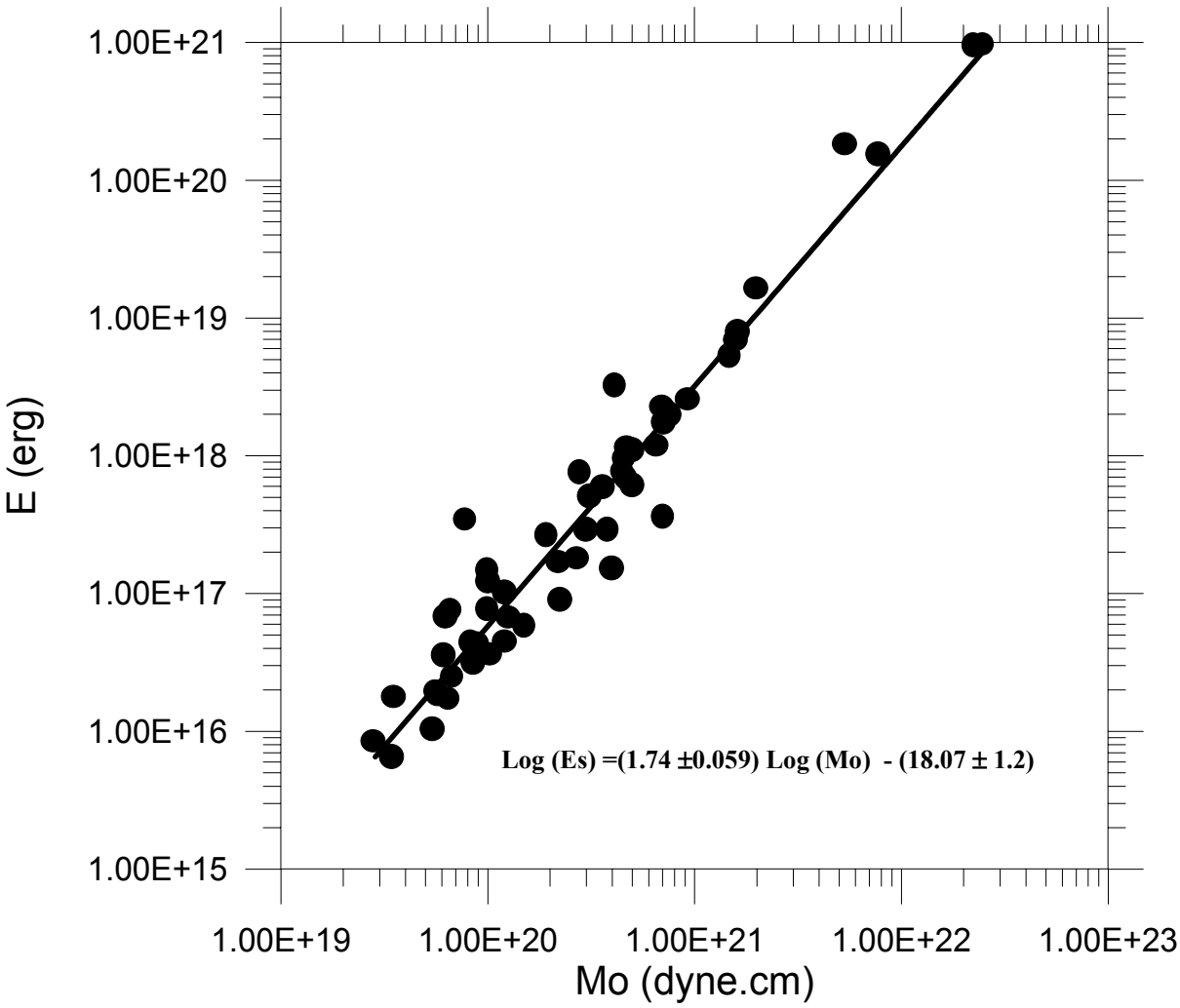

Fig(10) Radiated energy – Seismic moment relationship

Conclusions:

Seismic moment Mo, logarithm of the coda duration and the local magnitude empirical relations were derived for the aftershocks of 1992 Cairo earthquakes source area, providing a simple and straightforward way to qualify the source strength M0 through such relationships. The obtained relations are similar to those reported in other sites indicating that such relations may not change in different tectonic provinces.

The source estimates for the earthquakes with the seismic moment less than 10^{21} N.m. remain nearly constant. This tendency should be attributed to source effect. Similar situations have been observed in many regions where the stress drop decrease with decreasing seismic moment in this range.

The energy release was also calculated in this study. The Log Energy versus Log local magnitude and Log energy versus log moment was derived. The energy released versus magnitude is nearly the same as the expected theoretical value of Gutenberg and Richter, 1956 (Log Es=1.92 ML).

References:

Abu El Enein, K. M., H. M. Hussein, A. S. Abu El Ata and E.M. Ibrahim (2000): Seismological Aspects of the Cairo earthquake, 12 October 1992. Annali Di Geofisica V.43, N.3, 485-504.

Aki, K.(1988): Physical theory of earthquakes. In seismic hazard in the Mediterranean regions (J. Bonnin, M. Cara, A. Cisternas and R. Fancheti,eds) (Kluwer Academic Publishers, Dordrecht 1988) PP. 3-33.

Archuleta. R. J., Cranswick, E., Mueller, C. and Spudich, P. (1982) : Source parameters of the 1980 Mammoth lakes, California, Earthquake sequence, J. Geophys. Res. 87, 4595-4607.

Bakun, W. H. and Linda, A. G. (1977) : Local magnitudes, Seismic moments and Coda durations for earthquakes near Oroville, California. Bull. Seismol. Soc. Am. 67,615-629.

Boatwright, J. (1980): A spectral theory for circular seismic sources. Simple estimates of the source dimension, dynamic stress drop and radiated seismic energy. Bull. Seism. Soc. Am. 70, 1-27.

Boschi,E. Gardiani,D., Morelli,A., Romeo,G., and Taccentti, Q. (1988): Mednet-The Italian Broad-Band seismic Net-work for the Mediterranean . In : G.M. Purdy and A.M. Dziewonski (editors), Proc. Workshop on Broad-band down hole seismometers in the deep ocean. Wood holes oceanographic inst., Mass, pp.116-124.

Brune, J. N. (1970): tectonic stress and the spectra of seismic shear waves from earthquakes J. Geophys. Res., 75 :4997-5009.

Dessokey, M. M. Hussein H. M. Abdelrahman, E.S. and Abdelwahed, M. F. (2000): Local magnitude, duration magnitude and Seismic moment of Dahshour ,1992 earthquake. Annali Di Geofisica, V.43, N.1 95-105.

Dysart,P. S.,Snoke,J. A. and Sacks, I. S. (1988) : Source parameters and scaling relations for small earthquakes in the Matsushiro region, Southwest Honshu, Japan, Bull, Seismol. Soc. Am. 78,571-589.

Herrmann, R. B. (1974): Surface wave generation by Central United States earthquakes, Ph.D. Dissertation, Saint Louis University, St. Louis, Missouri.

Herrmann, R. B. and Kijko, A., (1983): Modeling some empirical vertical component Lg relations. Bull. Seismol. Soc. Am., 73,157-171.

Hussein, H. M. (1999): Source process of the October 12, 1992 Cairo Earthquake. Annali Di Geofisica, V.42 N. 4, August 1999.

Keilis-Borok, V. (1959): On estimation of the displacement in an earthquake source and of source dimension. Annali Di Geofisica, 12: 205-214.

Kim,W.Y., Wahlstrom R. and Uski,M. (1989): Regional spectral scaling relations of source parameters for earthquakes in the Baltic shield. Tectonophysics, 166:151-161.

Nuttli, O. W. (1986): Yield estimates of Nevada Test site explosions obtained from seismic Lg waves. J. Geophy. Res.,91 :2137-2151.

Street.R. L., Herrmann, R. B. and Nuttli, O. W., (1975): Spectral characteristics of the Lg wave generated by the central United States earthquakes. Geophys. J. R. Astron. Soc. 41: 51-63.

Valdes,C.M. and Meyer, R.P (1996): Spectral analysis and earthquake scaling of the petatan earthquake (Ms=7.6) aftershocks, recorded at stations along the pacific Coast and between the coast and mexico city. Pageoph, V.147, No. 4, 631-656.